Supplementary Information

A highly stable, selective, and high-performance VOC sensor using a SnS_2 nano-lotus structure

Rajneesh Kumar Mishra,[a] Gyu Jin Choi,[a] Yogendra Kumar Mishra,[b] Ajeet Kaushik,[c] Youngku Sohn,[d] Seung Hee Lee,*[e] Jin Seog Gwag*[a]

[a]Department of Physics, Yeungnam University, Gyeongsan, Gyeongbuk, 38541, South Korea.

[b]Mads Clausen Institute, NanoSYD, University of Southern Denmark, Alsion 2, 6400, Sønderborg, Denmark.

[c]NanoBioTech Laboratory, Department of Natural Sciences, Division of Sciences, Arts & Mathematics, Florida Polytechnic University, Lakeland, FL, 33805-8531, United States.

[d]Department of Chemistry, Chungnam National University, Daejeon, 34134, South Korea.

[e]Information Display/Energy Laboratory, Department of Nanoconvergence Engineering and Department of Polymer Nano-Science and Technology, Jeonbuk (Chonbuk) National University, Jeonju, Jeonbuk 54896, South Korea.

*Corresponding authors.

E-mail addresses: lsh1@jbnu.ac.kr (S. H. Lee); sweat3000@ynu.ac.kr (J. S. Gwag).

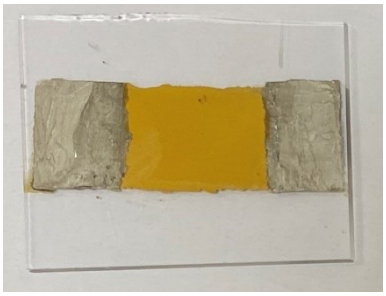

Fig. S1: Optical image of SnS_2 NLS gas sensor.

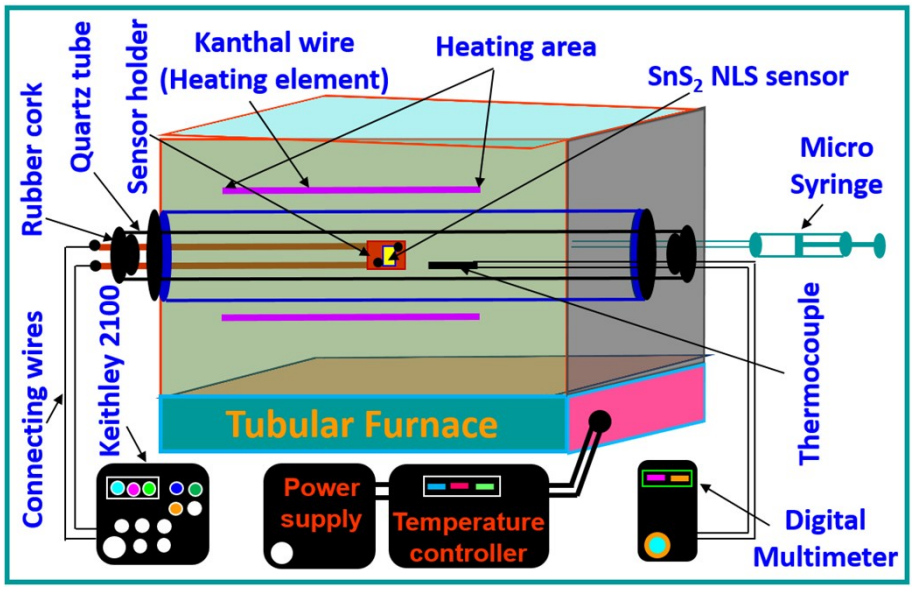

Fig. S2: Schematic view of gas sensing experimental setup.

The volume (V_{VOCs}) of liquid VOCs (μL) are calculated at a particular operating temperature and concentration (ppm) by using the following Eq. S1,[1]

$$V_{VOCs}\,(\mu L) = \frac{M_{VOCs}\,C_{ppm}\,PV}{\rho_{VOCs}\,RT} \tag{S1}$$

where M_{VOCs}, C_{ppm}, P, V, ρ_{VOCs}, R, and T are the molar mass, VOCs concentration, pressure, test chamber volume, the density of VOCs, the universal gas constant, and operating temperature, respectively.

The lattice spacing corresponding to an individual lattice of SnS_2 nano-lotus system (NLS) was calculated using Bragg's diffraction formula as discussed in Eq. S2,[2,3]

$$2d\sin\theta = n\lambda \tag{S2}$$

where d is lattice spacing (interplanar spacing), θ is Bragg's diffraction angle, n (= 1), λ is the wavelength of X-ray diffraction (here, Cu k_α = 1.54056 Å).

The lattice strain (ε) of SnS_2 NLS were evaluated using Eq. S3 (Tangent formula), respectively.[2,3]

$$\varepsilon = \frac{\beta}{4\tan\theta} \tag{S3}$$

where β and θ are the lattice spacing, X-ray wavelength, full width at the half maximum of the diffraction peaks, and Bragg's diffraction angle.

Table S1: Analysis of XRD results of the SnS_2 nano-lotus structure (NLS).

XRD analysis using experimental results					Lattice parameters using Rietveld refinement	JCPDS data 23-0677	
S. No.	2θ (º)	Lattice planes (*hkl*)	Lattice spacing (*d,* nm)	Lattice strain (ε)		Lattice spacing (*d,* nm)	Lattice parameters
1	15.0405	(001)	0.5885	0.0127	a (= b) = 3.6438 Å c = 5.9038 Å c/a = 1.6202	0.5890	a (= b) = 3.6486 Å c = 5.8992 Å c/a = 1.6168
2	28.3177	(100)	0.3148	0.0037		0.3162	
3	32.2069	(101)	0.2777	0.0058		0.2784	
4	41.9489	(102)	0.2151	0.0061		0.2155	
5	50.0970	(110)	0.1819	0.0031		0.1824	
6	52.5956	(111)	0.1738	0.0041		0.1743	
7	55.0366	(103)	0.1667	0.0048		0.1669	
8	60.7859	(201)	0.1522	0.0037		0.1526	

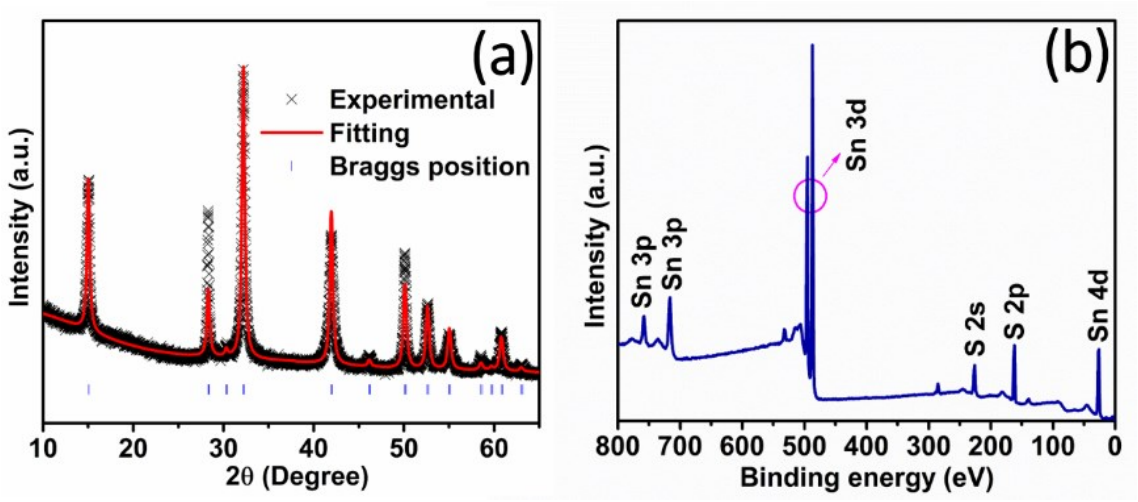

Fig. S3: (a) Rietveld refinement of XRD spectrum; and XPS survey spectrum of the SnS_2 NLS.

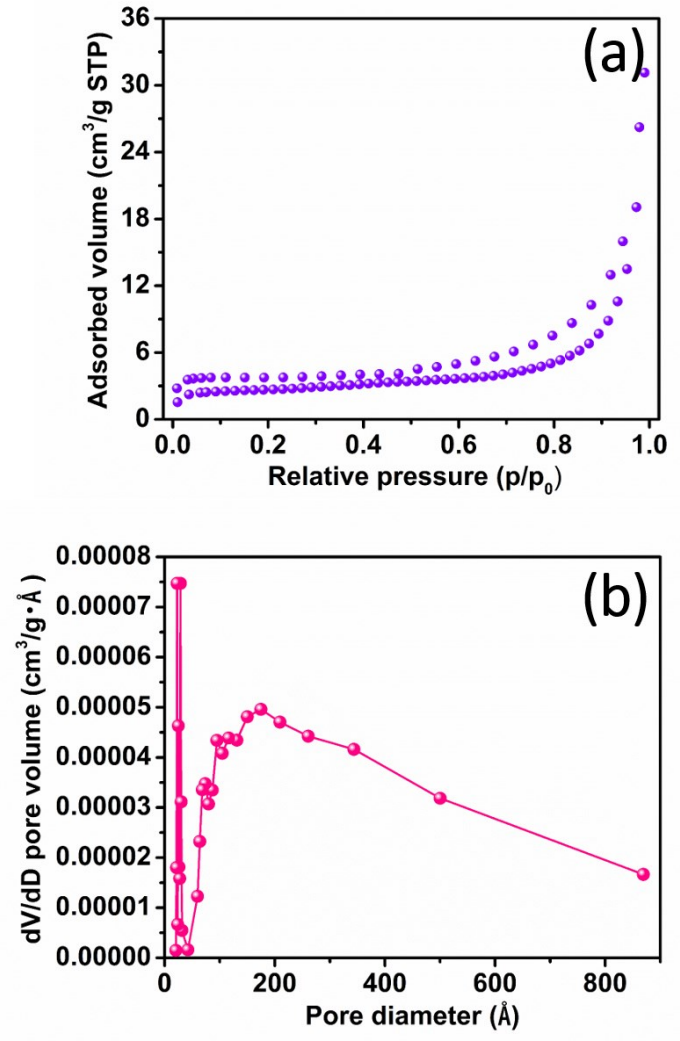

Fig. S4: (a) BET adsorbed volume *vs.* p/p_0 plot, (b) BJH dV/dD pore volume *vs.* pore diameter plot of SnS_2 NLS.

Table S2: BET surface area, BJH pore size, and volume analysis of SnS_2 NLS sensor.

	BET surface area	BJH pore size	BJH pore volume
lotus-like SnS_2	10.2304 m^2/g	Adsorption	Adsorption
		32.3905 nm	0.0459 cm^3/g

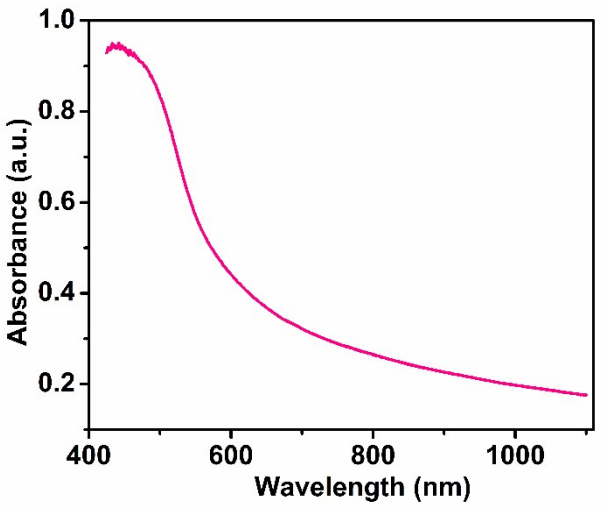

Fig. S5: UV-visible absorbance spectrum of SnS_2 NLS.

For the evaluation of energy bandgap by diffuse reflectance spectroscopy (DRS), the Kubelka-Munk equation is written in Eq. S4,[4,5]

$$\frac{K}{S} = \frac{(1-R)}{2R} = F(R) \quad \text{(S4)}$$

where *S, K,* and *R* are the scatterings, absorption coefficients, and reflectance, respectively, and F(*R*) is the Kubelka-Munk function. The optical bandgap and absorption coefficient α of a direct bandgap SnS_2 NLS are evaluated using the following Eq. S5,[4,5]

$$\alpha h\nu = C_1(h\nu - E_g)^{1/2} \quad \text{(S5)}$$

where α, hν, C_1, and E_g are the linear absorption coefficient of the material, photon energy, a proportionality constant, and optical bandgap, respectively.

The Kubelka-Munk absorption coefficient S is constant with wavelength when lotus-like SnS_2 diffusely scatters light and using the Eq. S5, we obtain the expression as written in Eq. S6,[4,5]

$$[F(R)h\nu]^2 = C_2(h\nu - E_g) \quad \text{(S6)}$$

Thus, by using Eq. S4 & S6, we can easily calculate the optical bandgap of SnS_2 NLS.

The Urbach energy is evaluated by using the following Eq. S7,[1,6]

$$\alpha = \alpha_o \exp\left(\frac{E}{E_U}\right) \quad \text{(S7)}$$

By using the Eq. S4 and Eq. S7, we can deduce the following relation Eq. S8,

$$F(R) = F(R)_o \exp\left(\frac{E}{E_U}\right) \quad \text{(S8)}$$

Therefore, we can easily estimate the Urbach energy of SnS_2 NLS using Eq. S8.

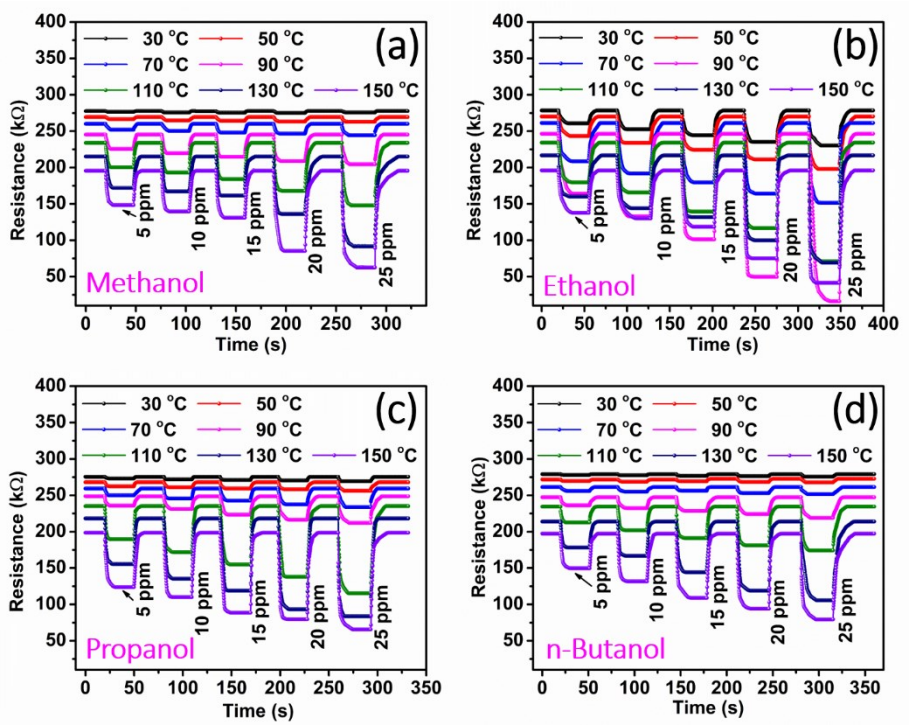

Fig. S6: (a-d) Dynamic gas sensing the resistance of SnS_2 NLS sensor to detect VOCs for various concentrations at different operating temperatures.

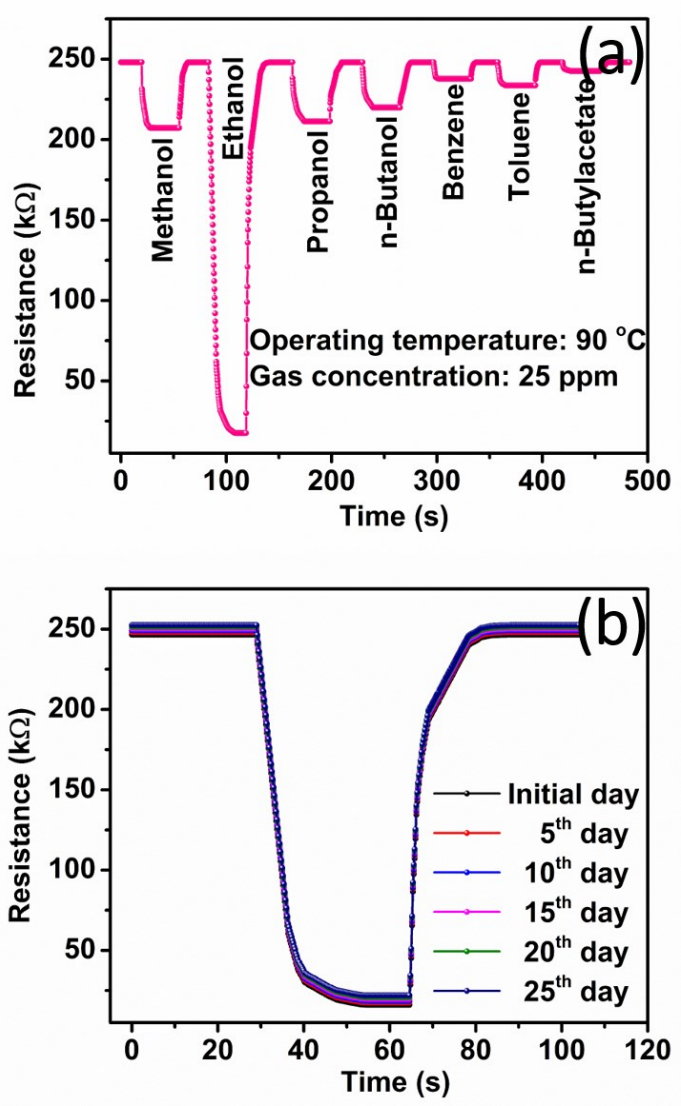

Fig. S7: Gas sensing resistance characteristics of SnS_2 NLS sensor; (a) selectivity for 25 ppm under various interfering gas at an operating temperature of 90 ^oC, and (b) stability test cycles for 25 ppm of ethanol concentration at 90 ^oC.

The selectivity coefficient of the SnS_2 NLS sensor was estimated by using the following Eq. S9;[7]

$$S_c = \frac{S_{ethanol}}{S_{interfering\ gas}} \quad \text{(S9)}$$

where S_c and $S_{\text{interfering gas}}$ are the sensitivities of SnS_2 NLS sensor to ethanol and other interfering gas, respectively, as listed in Table S3.

Table S3: Analysis of the selectivity coefficient of SnS_2 NLS sensor for 25 ppm concentration at an optimum operating temperature of 90 ^oC.

Sensing Element	**Interfering gas with 25 ppm concentration**					
lotus-like SnS_2 based ethanol sensor	Methanol	Propanol	n-Butanol	Benzene	Toluene	n-Butylacetate
	5.7	6.3	8.1	22.7	16.0	42.2

References

[1] S. B. Upadhyay, R. K. Mishra and P. P. Sahay, Enhanced acetone response in co-precipitated WO_3 nanostructures upon indium doping, Sens. Actuators, B, 2015, 209, 368-376.

[2] B. D. Cullity, Elements of X-ray Diffraction, Addison-Wesley, New York, 1978.

[3] H. P. Klug and L. E. Alexander, X-ray Diffraction Procedures for Polycrystalline and Amorphous Materials, Wiley, New York, 1974.

[4] C. Wu, D. Guo, P. Li, S. Wang, A. Liu and F. Wu, A study on the effects of mixed organic cations on the structure and properties in lead halide perovskites, Phys. Chem. Chem. Phys., 2020, **22**, 3105-3111.

[5] J. Torrent and V. Barron, Diffuse Reflectance Spectroscopy of Iron Oxides, Encycl. Surf. Colloid Sci., 2002, 1438-1446.

[6] P. Chetri and A. Choudhury, Investigation of optical properties of SnO_2 nanoparticles, Physica E, 2013, **47**, 257-263.

[7] M. Siemons and U. Simon, Gas sensing properties of volume-doped $CoTiO_3$ synthesized via polyol method, Sens. Actuators, B, 2007, **126**, 595-603.